ARTICLE

Genomic profiling of primary histiocytic sarcoma reveals two molecular subgroups

Caoimhe Egan,[1] Alina Nicolae,[1] Justin Lack,[2] Hye-Jung Chung,[1] Shannon Skarshaug,[1] Thu Anh Pham,[1] Winnifred Navarro,[1] Zied Abdullaev,[1] Nadine S. Aguilera,[3] Liqiang Xi,[1] Svetlana Pack,[1] Stefania Pittaluga,[1] Elaine S. Jaffe[1] and Mark Raffeld[1]

[1]Laboratory of Pathology, National Cancer Institute, National Institutes of Health, Bethesda, MD; [2]NIAID Collaborative Bioinformatics Resource (NCBR), National Institute of Allergy and Infectious Diseases, National Institutes of Health, Bethesda, MD and [3]University of Virginia Health System, Charlottesville, VA, USA

Ferrata Storti Foundation

Haematologica 2020
Volume 105(4):951-960

ABSTRACT

Histiocytic sarcoma is a rare malignant neoplasm that may occur *de novo* or in the context of a previous hematologic malignancy or mediastinal germ cell tumor. Here, we performed whole exome sequencing and RNA-sequencing (RNA-Seq) on 21 archival cases of primary histiocytic sarcoma. We identified a high number of genetic alterations within the RAS/RAF/MAPK pathway in 21 of 21 cases, with alterations in *NF1* (6 of 21), *MAP2K1* (5 of 21), *PTPN11* (4 of 21), *BRAF* (4 of 21), *KRAS* (4 of 21), *NRAS* (1 of 21), and *LZTR1* (1 of 21), including single cases with homozygous deletion of *NF1*, high-level amplification of *PTPN11*, and a novel *TTYH3-BRAF* fusion. Concurrent *NF1* and *PTPN11* mutations were present in 3 of 21 cases, and 5 of 7 cases with alterations in *NF1* and/or *PTPN11* had disease involving the gastrointestinal tract. Following unsupervised clustering of gene expression data, cases with *NF1* and/or *PTPN11* abnormalities formed a distinct tumor subgroup. A subset of *NF1/PTPN11* wild-type cases had frequent mutations in B-cell lymphoma associated genes and/or clonal IG gene rearrangements. Our findings expand the current understanding of the molecular pathogenesis of this rare tumor and suggest the existence of a distinct subtype of primary histiocytic sarcoma characterized by *NF1/PTPN11* alterations with predilection for the gastrointestinal tract.

Introduction

Histiocytic sarcoma (HS) is a rare and aggressive malignant neoplasm that has morphological and immunophenotypic features of mature tissue histiocytes.[1] It predominantly occurs in adulthood, although any age may be affected. Sites of involvement may be nodal or extranodal, and include the gastrointestinal (GI) tract, skin, and liver.[2] Histologically, the tumor cells are usually pleomorphic with cytologic atypia and can be multinucleated or have a spindled or xanthomatous morphology. The diagnosis of HS requires the demonstration of histiocytic markers (CD68, CD163, CD4 or lysozyme) and the exclusion of tumors of other lineages by negativity of immunohistochemical stains for Langerhans cells (CD1a, langerin), follicular dendritic cells (CD21, CD23, clusterin), B and T cells, cells of myeloid or epithelial lineage (MPO, CK), and melanocytic markers.[3,4]

Histiocytic sarcoma may arise as a primary neoplasm (pHS), but is also well described in the context of an existing or concurrently diagnosed hematologic malignancy, most frequently a follicular lymphoma, but also chronic lymphocytic leukemia (CLL) and B- or T-lymphoblastic leukemia (B-ALL/T-ALL).[5-9] Rare cases have also been associated with mediastinal germ cell tumor.[3] Cases arising in the context of a lymphoid neoplasm are often referred to as "secondary" HS (sHS), and frequently possess identical clonal antigen receptor gene rearrangements or occasionally identical structural events (e.g. identical IGH/*BCL2* rearrangements) as in the associated lymphoma. However, on histological and immunophenotypic

Correspondence:

MARK RAFFELD
mraff@mail.nih.gov

Received: June 25, 2019.

Accepted: August 21, 2019.

Pre-published: August 22, 2019.

doi:10.3324/haematol.2019.230375

Check the online version for the most updated information on this article, online supplements, and information on authorship & disclosures: www.haematologica.org/content/105/4/951

examination they have no other evidence of lymphoid origin.[5,6,10] Rather, these cases express markers of histiocytic/monocytic differentiation, but are nonetheless thought to be related to the associated B-cell neoplasm through a poorly understood process sometimes referred to as transdifferentiation[5] or origin from a common neoplastic progenitor.[11] Interestingly, the presence of clonal IG gene rearrangements or a *BCL2* translocation is not restricted to secondary cases associated with a B-cell malignancy, as both abnormalities have also been observed in sporadic or "primary" cases of HS.[12,13]

In contrast to the more comprehensive studies performed in other histiocytic tumors, especially Langerhans cell histiocytosis and Erdheim-Chester disease,[14-17] until recently, molecular analysis of HS has remained relatively underexplored.[18] *BRAF* p.V600E mutations have been reported in approximately 12% of 108 published cases with molecular or immunohistochemical data, and additional alterations in members of the RAS/MAPK and PI3K/AKT pathways, including other *BRAF* variants, *KRAS, HRAS, NRAS, MAP2K1, PIK3CA, PTPN11* and *PTEN* are also described (see *Online Supplementary Tables S1* and *S2* for a complete list of references). The distinction between pHS and sHS is often not clearly defined in these studies. To better understand the genetic landscape of alterations in a well-characterized series of pHS, we performed an integrated genomic analysis of 21 cases utilizing whole exome sequencing, whole transcriptome sequencing, and copy number analysis. Cases of sHS were intentionally excluded from this study.

Methods

Case selection, IGH/*BCL2* and clonality studies

Twenty-one cases of pHS were identified from the files of the Hematopathology Section of the National Cancer Institute under an Institutional Review Board approved protocol (*Online Supplementary Methods*). The histological and immunophenotypic features and clonality characteristics of the cases are detailed in Figure 1 and *Online Supplementary Table S3*. DNA and RNA were isolated from formalin-fixed paraffin embedded (FFPE) tissue. Immunoglobulin (IGH and IGK) and T-cell receptor (TRG) gene rearrangement studies were performed in 19 of 21 cases and IGH/*BCL2* (MBR) translocation analysis in 17 of 21 cases (*Online Supplementary Methods*).

Whole exome sequencing

Samples were sequenced in two groups: an initial cohort of 15 tumor samples with two matched normal samples on an Illumina HiSeq2500 with TruSeq V4 chemistry and a subsequent cohort of six tumor samples with one matched normal sample on an Illumina HiSeq3000 with TruSeq V2 chemistry (Illumina, San Diego, CA, USA). Alignment and variant calling were performed following the Center for Cancer Research Collaborative Bioinformatics Resource (CCBR) pipeline (*https://github.com/CCBR/Pipeliner*) as described in the *Online Supplementary Methods*.

Variant analysis

Germline variants were excluded in three cases with available matched normal samples. Exonic variants with a depth of coverage ≥ 20 and a read count ≥ 6 were retained. As matched germline samples were unavailable for most cases, we generated a targeted gene list to reduce the number of variants for review. Genes were compiled from the COSMIC Cancer Gene Census (*http://cancer.sanger.ac.uk*)[19] and literature review to select disease relevant genes with a potential oncogenic role. The list was supplemented with additional genes identified by filtering the exome sequencing data to include recurrently mutated genes (≥ 3 samples) after removing variants based on CADD phred-like scores[20] and population allele frequencies (*Online Supplementary Methods*). All variants involving genes in the targeted gene list were evaluated and categorized as significant based on set criteria (*Online Supplementary Methods* and *Online Supplementary Figure S1*). Variants not meeting the set criteria were excluded. Mutations were reviewed in the Integrative Genomics Viewer (IGV).[21]

RNA sequencing

Details of RNA library preparation, sequencing and fusion detection are described in the *Online Supplementary Methods*. RNA-Seq analysis was conducted using the CCBR RNA-Seq pipeline *(https://github.com/CCBR/Pipeliner*). Gene set enrichment analysis was performed using Ensemble of Gene Set Enrichment Analyses (EGSEA data version: 1.6.0)[22] and sorted by average rank.

Copy number analysis

Nine samples were successfully assessed using the OncoScan CNV FFPE Assay (Affymetrix, Santa Clara, CA, USA) according to the manufacturer's protocol. Copy number was estimated from the exome sequencing data in the remaining cases using default settings for CNVkit v0.8.5[23] and PureCN v1.8.1.[24] Calls from CNVkit were exported in nexus.ogt format for review and annotation in Nexus 9.0 Software (BioDiscovery, Hawthorne, CA, USA). Alterations called by both algorithms were further analyzed as described in the *Online Supplementary Methods*.

Data sharing

All genomic data from this study will be deposited in the dbGaP database (*www.ncbi.nlm.nih.gov/gap*) with the accession number phs001748.v1.p1.

Results

Primary histiocytic sarcoma is characterized by frequent alterations involving the RAS/MAPK pathway

Whole exome sequencing was performed on 21 cases of pHS as defined in the *Online Supplementary Methods*, and on three matched normal controls (His01, His08, His16), in two groups. The median coverage in the first 15 cases ranged from 106-165x, and in the second six cases from 205-305x. Sequencing depth for the three matched controls ranged from 72-143x. Variants were filtered as described in the *Online Supplementary Methods* using stringent criteria, and all candidates were individually reviewed in IGV.

Multiple and occasionally concurrent mutations involving genes of the RAS/MAPK pathway (Figure 2, *Online Supplementary Table S4* and *Online Supplementary Figure S2*) were identified in 19 of the 21 cases. The most frequently mutated RAS/MAPK pathway genes were *NF1* and *MAP2K1* (5 cases each). Interestingly, 4 of 5 cases with *NF1* mutations involved the GI tract, although one biopsy sequenced was a supraclavicular lymph node. Three of the cases had a single *NF1* mutation (p.Q1822* [His01]; p.V1182D [His02]; p.Q1086* [His16]), whereas the other two had two mutations each (p.R304* and p.Q1775* [His12]; p.L298* and p.K660fs [His17]). Six of the seven variants were nonsense mutations or frameshift deletions

and therefore predicted to be inactivating. The single missense mutation (p.V1182D) was predicted to be deleterious or probably damaging by functional impact algorithms SIFT[25] and PolyPhen-2.[26] In addition to *NF1* mutations, 3 of the 5 cases showed concurrent mutations in *PTPN11* (p.F71V [His01]; p.E76G [His02]; p.A72V [His12]). *PTPN11* mutations were present within the autoinhibitory N-SH2 domain at amino acid residues known to be associated with a gain-of-function consequence and described in Noonan syndrome and juvenile myelomonocytic leukemia (JMML).[27,28] One case without a *PTPN11* mutation [His17] had an additional mutation in *GNAI2* at p.R179H, a codon previously shown to be targeted by activating mutations[29] and 1 of the 5 *NF1* mutated cases also had a mutation in *JAK2* at p.V617F [His12]. A fourth *PTPN11* mutated case at p.E76K [His18] did not have another RAS pathway mutation; however, it had high level amplification of the mutated *PTPN11* allele (*see below*).

Additional mutations involving the RAS/MAPK pathway were detected in another 13 cases, none of which had

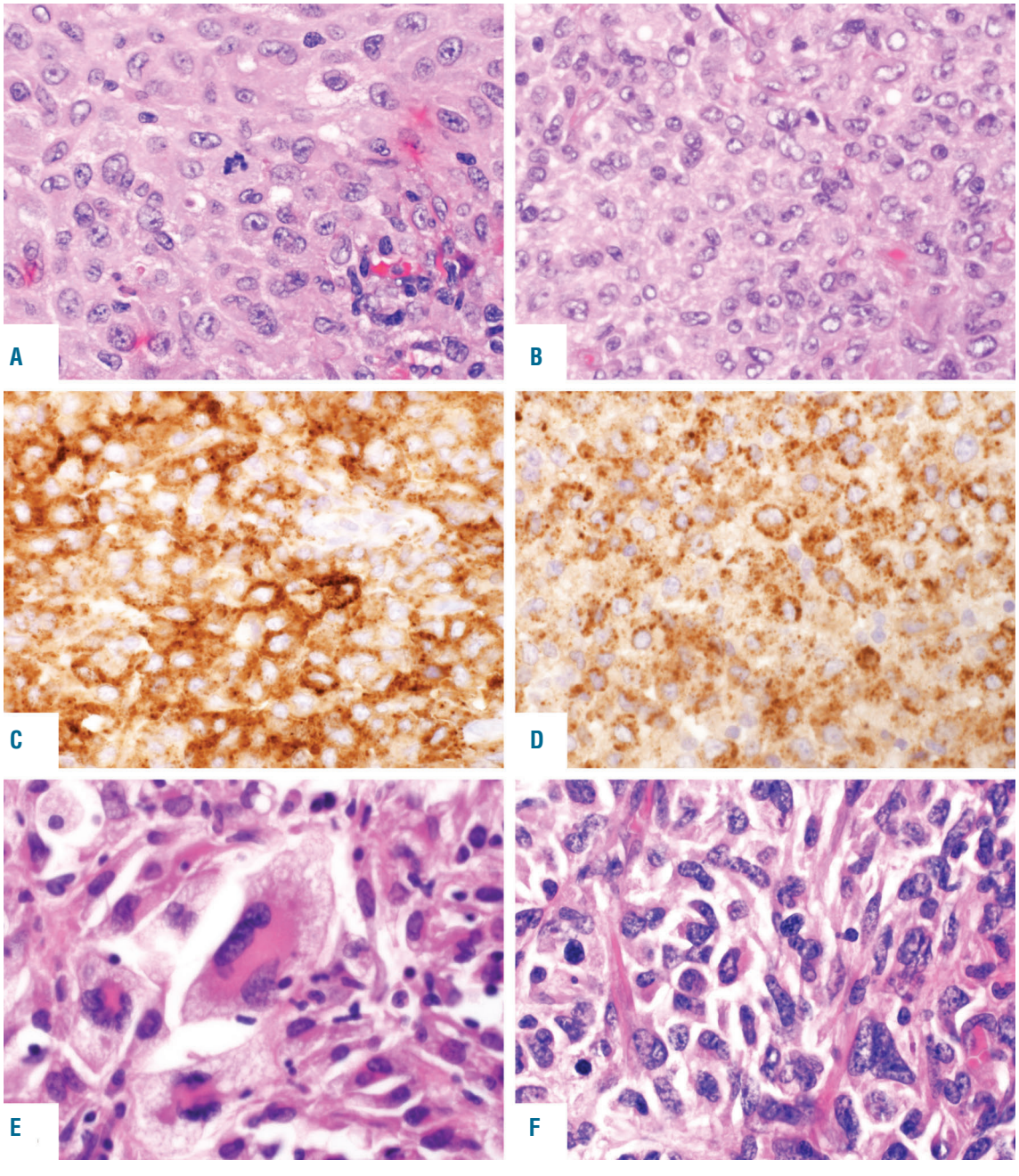

Figure 1. Histological features of primary histiocytic sarcoma (pHS). Cases involving lymph node (A) and tonsil (B) showing moderate nuclear atypia and abundant eosinophilic cytoplasm; Hematoxylin & Eosin (H&E) staining, original magnification x400. The cells express (C) CD163; original magnification x400 and (D) CD68; original magnification x400. (E and F) Two extranodal (gastrointestinal tract) cases showing marked nuclear pleomorphism, multinucleated cells and foam cells; H&E stain, original magnification x400.

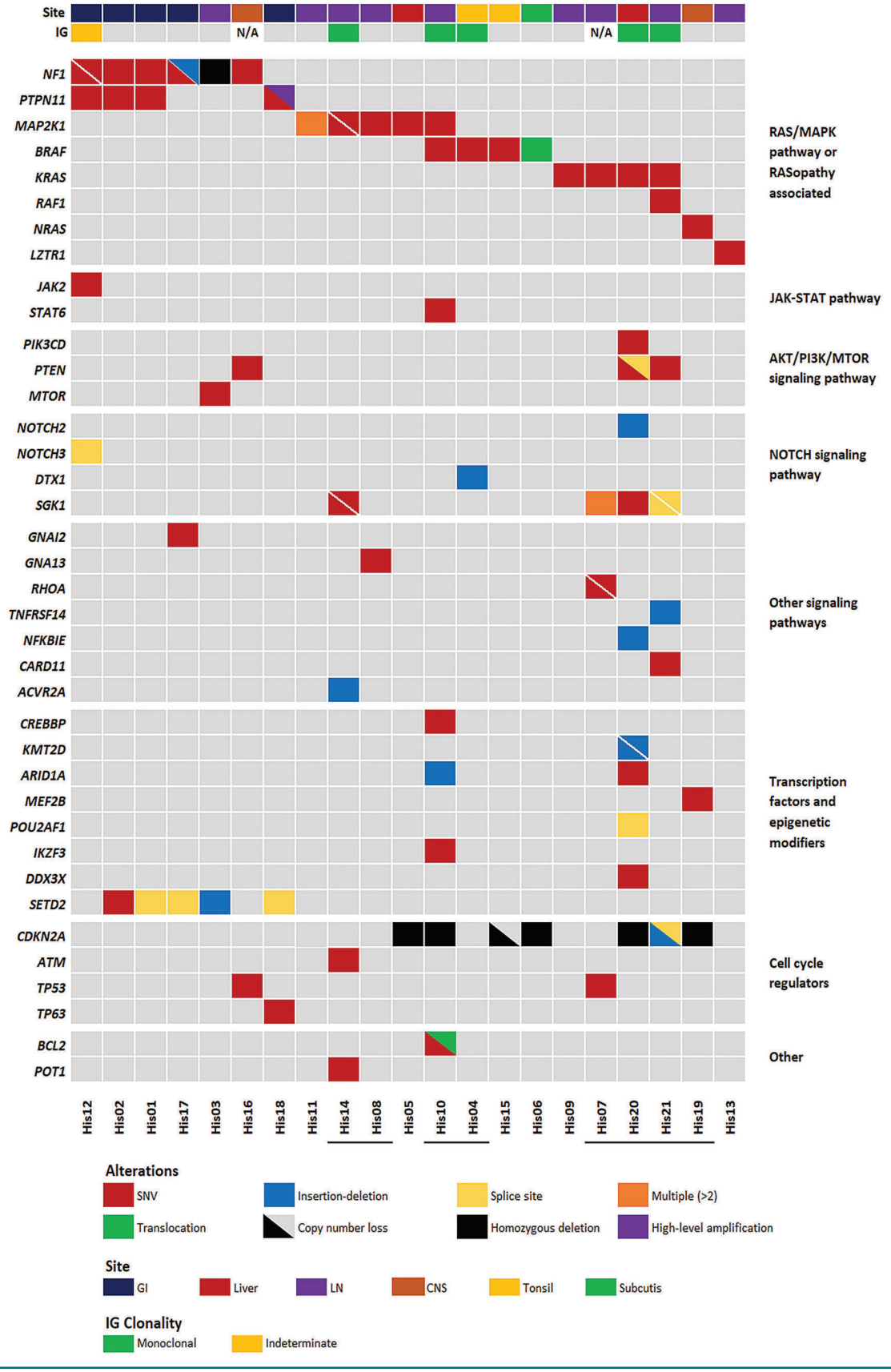

Figure 2. Selected molecular alterations in primary histiocytic sarcoma (pHS) cases. Genes are listed in the rows and organized by pathway or function. Samples are listed in columns. Site and IG gene rearrangement status are indicated in the top annotation bar. Underlined sample labels indicate a case with a B-cell lymphoma associated mutation or clonal IG gene rearrangement. Annotated focal copy number alterations and translocations were detected by OncoScan and/or verified by fluorescence *in situ* hybridization or polymerase chain reaction. GI: gastrointestinal tract; LN: lymph node; CNS: central nervous system.

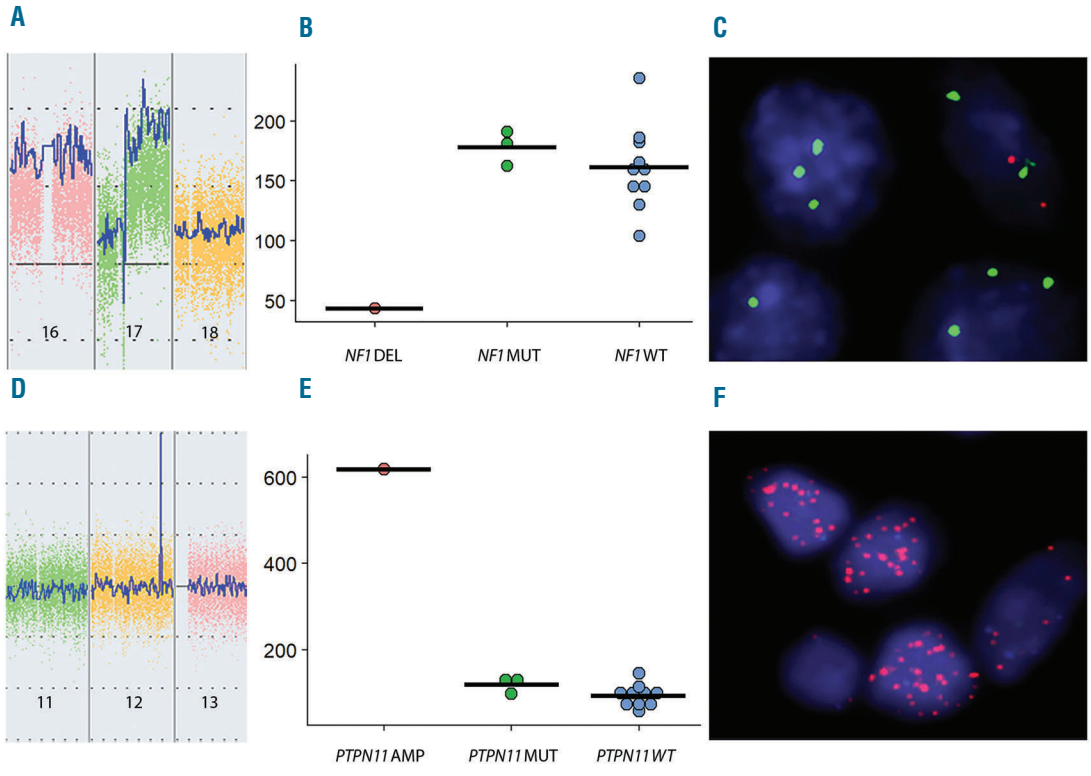

Figure 3. *NF1* homozygous deletion. (A) Inverted peak in chromosome 17 consistent with homozygous deletion of *NF1* (ChAS 3.3). (B) Reduction in *NF1* transcript in the case with homozygous deletion (DEL) compared with *NF1* mutated (MUT) and wild-type (WT) cases [normalized RNA-sequencing (RNA-Seq) count data]. (C) Fluorescence *in situ* hybridization (FISH) showing multiple copies of the CEP 17 probe (green) with loss of the *NF1* probe (orange) (D-F). *PTPN11* amplification. (D) Peak in chromosome 12 consistent with high-level amplification of *PTPN11* (ChAS 3.3). (E) Increased *PTPN11* transcript in the amplified (AMP) case compared with *PTPN11* mutated (MUT) and wild-type (WT) cases (normalized RNA-Seq count data). (F) FISH showing multiple copies of the *PTPN11* gene (orange) in a double minute pattern.

NF1 or *PTPN11* mutations. *MAP2K1* mutations were present in five cases and involved known hotspot regions in exons 2 and 3, the negative regulatory region (p.F53L [His10, His14]; p.K57E [His05]) and the catalytic core domain (p.I103N [His14]; p.C121S [His08, His11]).[30] As well as the mutation at p.C121S, case [His11] had two additional *MAP2K1* mutations at p.Y125C and p.R181K. The functional consequences of these mutations are not known; however, the p.Y125C substitution also involved the catalytic core domain in the same allele as the pathogenic p.C121S mutation. One case with a *MAP2K1* mutation had a co-occurring non-canonical *BRAF* mutation (p.G469V [His10]) and two additional cases had *BRAF* p.V600E [His04 and His15] mutations. Pathogenic *KRAS* mutations were detected in four cases (p.G12D [His21]; p.G12C [His09]; p.Q61H [His07] and p.A146V [His20]), one of which, [His21] also had a mutation in *RAF1* (p.D486G). A single case had an *NRAS* mutation at p.Q61R [His19]. Finally, a mutation in *LZTR1* (p.R118H) was identified in case [His13]. *LZTR1* encodes an adaptor for CUL3 ubiquitin ligase complexes[31] and is implicated in Noonan syndrome,[32,33] malignancy[31] and schwannomatosis.[34] Mutations in *LZTR1* have recently been shown to dysregulate RAS ubiquitination leading to increased RAS activity.[35] The p.R118H mutation affects a conserved residue in the Kelch domain and is reported once in the COSMIC database. Mutations in *LZTR1* are not typically associated with histiocytic tumors. This case met our inclusion criteria, but notably had some atypical features including aberrant expression of perforin and CD7 and a clonal TRG gene rearrangement.

Mutations involving the PI3K pathway were identified in four cases, including two with *KRAS* mutations and two with *NF1* alterations, with mutations identified in *PTEN* (p.Q171* [His16]; p.D24H and c.79+1G>C [His20] and p.L140* [His21]), *PIK3CD* (p.E1021K [His20]) and *MTOR* (p.I2501F [His03]). Additional mutations in genes previously reported to be mutated in B-cell lymphomas were detected in *SGK1* (p.R285K, p.I238T, p.H237Y, p.K213R and p.P147S [His07]; p.E162G and p.K136R [His14]; p.Q125H [His20]; c.437+1G>A and c.362-1G>A [His21]), *NOTCH2* (p.I2304fs [His20]), *DTX1* (p.W37* [His04]), *TNFRSF14* (p.T169fs [His21]), *CARD11* (p.R179Q [His21]), *NFKBIE* (p.L410fs [His20]), *GNA13* (p.F4V [His08]), *POT1* (p.R273W [His14]) and *BCL2* (p.E136D [His10]).[36-40]

In addition to mutations in the signaling pathways described above, mutations in epigenetic modifiers and/or transcription factors were detected in eight cases, including five with *SETD2* mutations (c.7432-2A>C [His01]; p.V1820E [His02]; p.P132fs [His03]; c.4715+1G>T [His17] and c.7432-1G>A [His18]), two with *ARID1A* mutations (p.L2011fs [His10] and p.G2087R [His20]) and single cases with *CREBBP* (p.Y1433C [His10]), *KMT2D* (p.E2225fs and p.K1752fs [His20]), *DDX3X* (p.V206M [His20]), *POU2AF1* (c.16+2T>G [His20]), *IKZF3* (p.L162R [His10]), *STAT6*

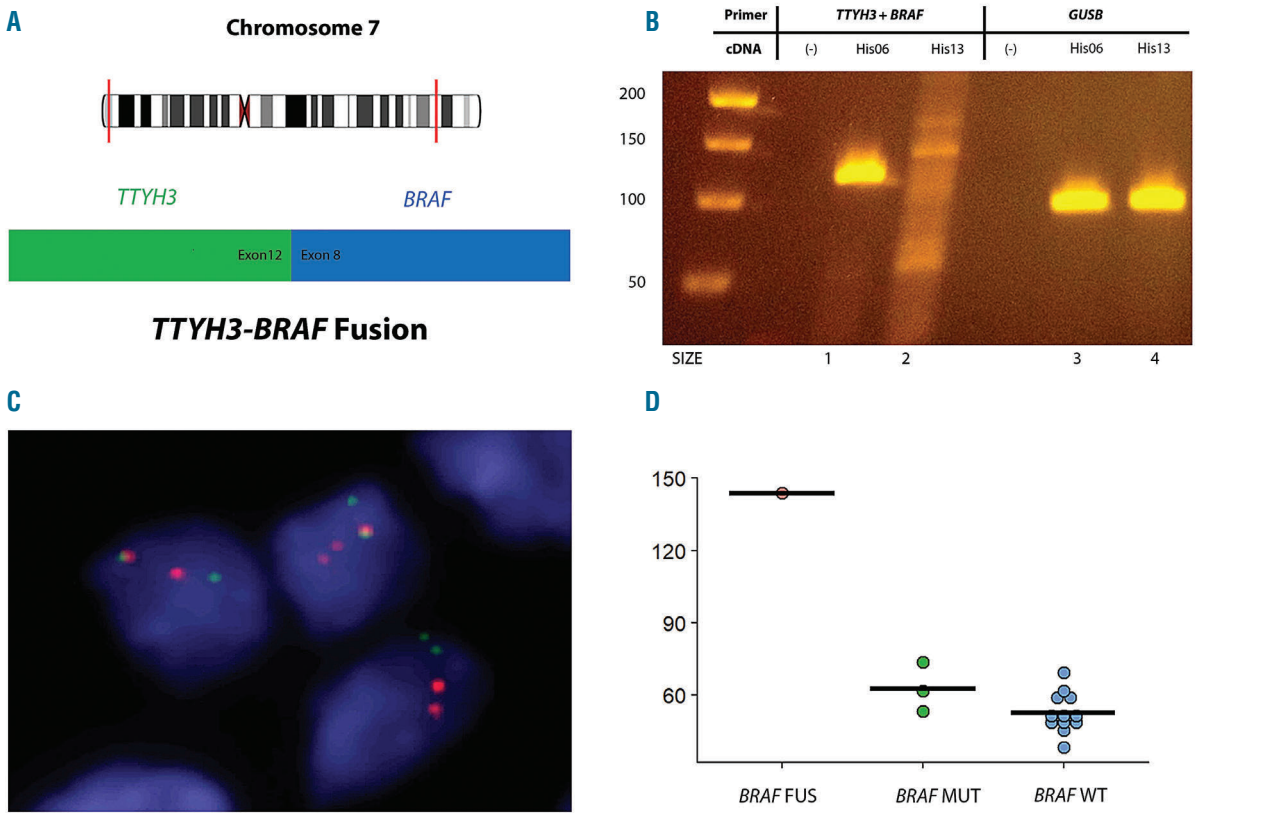

Figure 4. *TTYH3-BRAF* fusion. (A) Diagram of the intrachromosomal fusion on chromosome 7 of *TTYH3* (exon 12) to *BRAF* (exon 8). (B) Gel electrophoresis of the reverse transcription polymerase chain reaction confirming the presence of the *TTYH3-BRAF* fusion in Lane 1. (Lane 2 – Negative control; Lanes 3 and 4 – Positive controls). (C) Demonstration of split signals by fluorescence *in situ* hybridization, indicating a *BRAF* translocation (*BRAF* break apart probe, orange – 3'; green – 5'). (D) Increased *BRAF* transcript in the case with the fusion (FUS) compared with *BRAF* mutated (MUT) and wild-type (WT) cases (normalized RNA-Seq count data).

(p.D419G [His10]) and *MEF2B* (p.R64H [His19]) mutations. *SETD2* mutations were exclusive to the *NF1/PTPN11* mutated group, including one case found to have homozygous deletion of *NF1* and one case with *PTPN11* gene amplification (both described below), while the *ARID1A, CREBBP, KMT2D, DDX3X, IKZF3, STAT6* and *MEF2B* mutations were present in the *NF1/PTPN11* wild-type group. Known pathogenic mutations in *TP53* were identified in 2 of 21 cases (p.G245S [His07]; p.R175H [His16]).

Copy number analysis shows additional alterations in *NF1, PTPN11* and *CDKN2A*

A homozygous deletion in the *NF1* gene was identified in an additional case [His03] from a lymph node and confirmed using a fluorescence *in situ* hybridization (FISH) probe targeting the deleted area. RNA-Seq data showed markedly lower counts of *NF1* transcript in this case in comparison to the other samples, consistent with loss of *NF1* (Figure 3A-C). The three cases with a single *NF1* mutation [His01, His02 and His16] showed loss-of-heterozygosity (LOH) or copy number loss involving chromosome 17 including the *NF1* gene.

Interestingly, a focal high-level amplification in chromosome 12 targeting *PTPN11* was discovered in a further case [His18] involving the GI tract. This case harbored a known variant in the N-SH2 domain (p.E76K) of the amplified *PTPN11* allele. In contrast to the other *PTPN11* mutated cases, no mutation of *NF1* was detected by exome sequencing. This high-level amplification was confirmed by FISH which showed multiple copies of the *PTPN11* gene in the tumor cells in a double minute pattern. The amplified segment involved the entire *PTPN11* gene, with the breakpoints identified by OncoScan in an adjacent gene, *RPH3A*, and 5' to *PTPN11* involving *HECTD4* on the complementary strand. This event was associated with a dramatic increase in *PTPN11* transcripts in comparison to the other cases (Figure 3D-F).

Cases with *NF1/PTPN11* alterations had associated losses or LOH of chromosome 10 or 10q and chromosome 17 or 17p in 3 of 5 cases assessed by OncoScan [His01, His02, His12] and confirmed by FISH in two cases (*Online Supplementary Figure S3A-C*). Focal *CDKN2A* losses were present by OncoScan or confirmed by FISH in six cases that were *NF1/PTPN11* wild-type [His05, His06, His10, His15, His19, His20] and included five cases with homozygous deletion [His05, His06, His10, His19, His20]. All homozygous deletions were confirmed by FISH (*Online Supplementary Figure S3D and E*). Both *TP53* mutated cases had LOH involving the gene, with one *NF1* mutated case [His16, not assessed by OncoScan] showing a near-haploid genome with loss of chromosome 17 and the second case [His07] showing LOH at chromosome 17p.

Identification of a novel *TTYH3-BRAF* fusion

Fusion calling of RNA-Seq data identified a novel intrachromosomal fusion transcript between exon 12 of

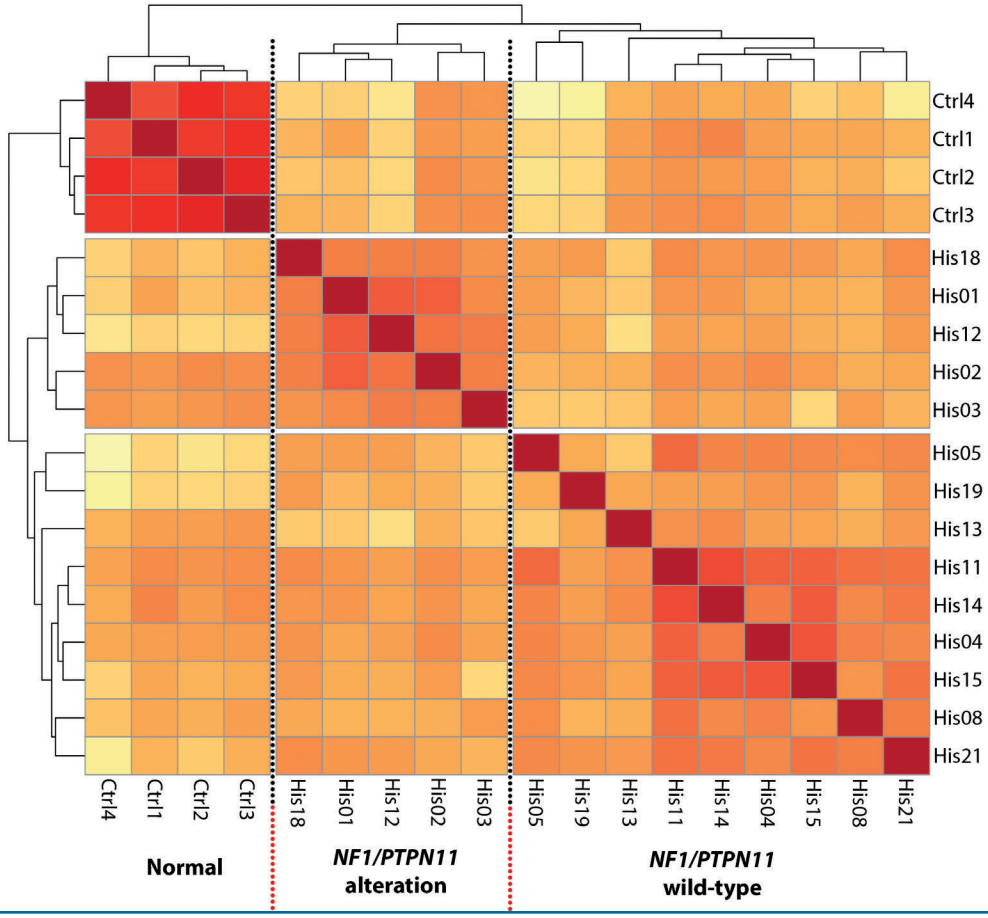

Figure 5. Exploratory analysis of RNA-sequencing (RNA-Seq) data. Unsupervised clustering based on transcriptome-wide gene expression and using Euclidean distance with complete linkage identifies three clusters corresponding to the normal samples, tumor samples with alterations in *NF1/PTPN11* and the remaining *NF1/PTPN11* wild-type tumor samples.

TTYH3 and exon 8 of *BRAF* on chromosome 7 in a case without any other known driver mutation [His06]. This novel *TTYH3-BRAF* fusion has a similar structure to other reported *BRAF* fusions,[41,42] with replacement of the RAS-binding domain of *BRAF* by a 5' fusion partner, in this case, a chloride ion channel gene, *TTYH3* (Figure 4A). The presence of the fusion transcript was confirmed by reverse transcription polymerase chain reaction (RT-PCR) using primers for exon 12 of *TTYH3* and exon 8 of *BRAF* (Figure 4B), as well as by FISH (Figure 4C). Interestingly, RNA-Seq data showed markedly higher levels of *BRAF* transcript as compared to all other samples, suggesting that the *TTYH3* gene partner contributed an active promoter to the fusion gene (Figure 4D). *TTYH3* was found to be highly expressed in all cases with RNA-Seq data (*data not shown*).

Identification of two primary histiocytic sarcoma subgroups by whole transcriptome sequencing: association with *NF1/PTPN11* mutational status

We examined the gene expression profile of pHS through whole transcriptome sequencing of 17 of the tumor samples using four cases of reactive nodal histiocytic infiltrates as controls. Three of the 17 tumor samples initially sequenced were excluded from the differential expression analysis as they failed quality control metrics and/or were outliers within the tumor group [His10] or within the data as a whole [His06, His09] (*Online Supplementary Figure S4*). Re-clustering segregated the remaining samples into three groups: normal controls (4 samples), cases with *NF1* or *PTPN11* abnormalities (5 samples), and a third heterogeneous group comprising *NF1/PTPN11* wild-type cases (9 samples) (Figure 5).

Gene set enrichment analysis shows enrichment of cell cycle processes in cases without *NF1/PTPN11* abnormalities

To better understand the potential biological significance of the two pHS subgroups, we performed gene set enrichment analysis using EGSEA. This analysis showed significant enrichment of cell cycle pathway and cell proliferation gene sets in the *NF1/PTPN11* wild-type tumor samples relative to samples with *NF1/PTPN11* alterations. Ki67 immunohistochemistry was performed on a subset of cases and confirmed the lower proliferation rate in the *NF1/PTPN11* subgroup (Figure 6 and *Online Supplementary Table S3*).

The two tumor subgroups were also evident in the differential expression analysis comparing the normal and tumor samples when the genes with significant differential expression (FDR < 0.05, absolute log fold change > 1) were visualized across samples (*Online Supplementary Table S5* and *Online Supplementary Figure S5*). We took advantage of this to explore the possibility that disease site might be influencing the clustering of the tumor sub-

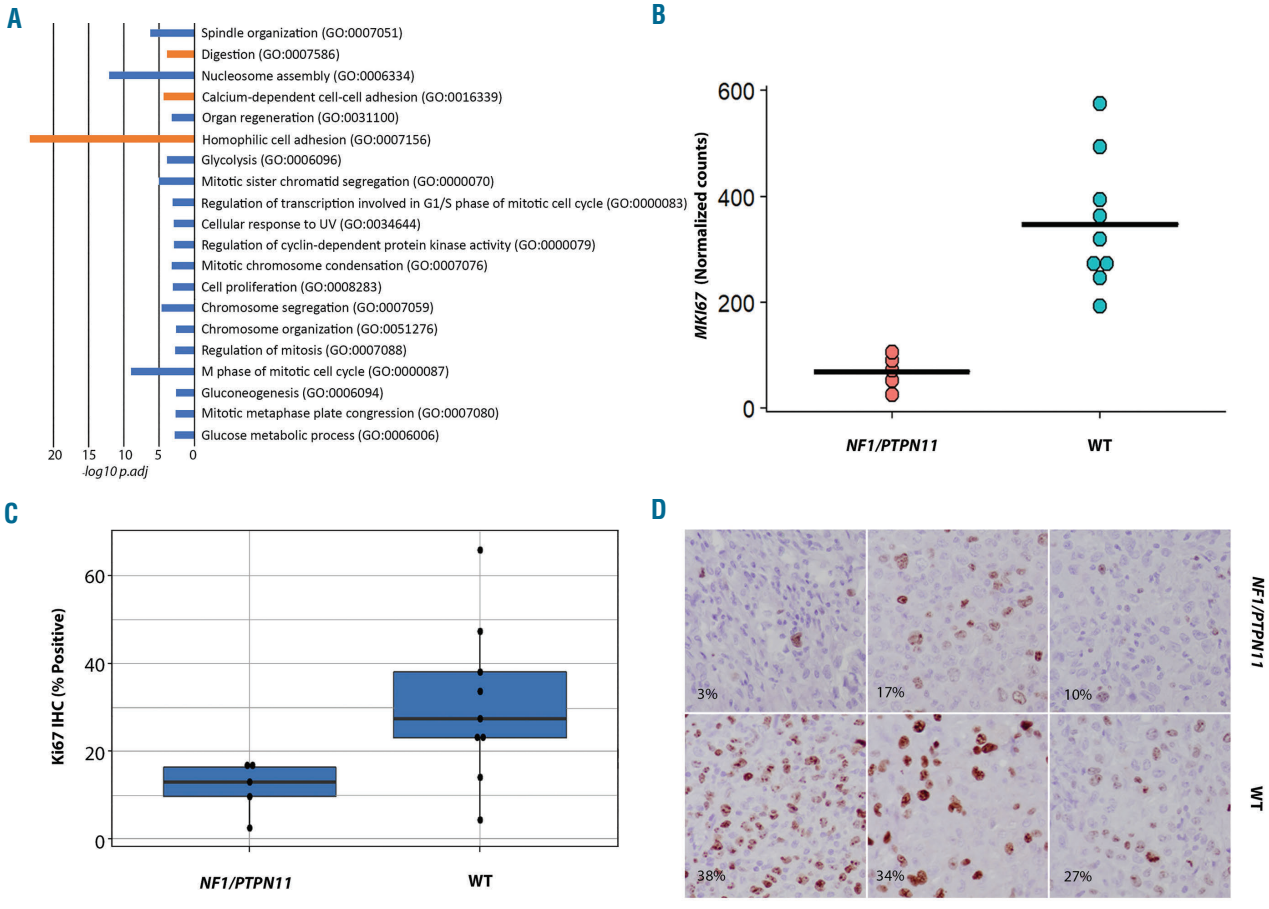

Figure 6. Cell cycle and proliferation. (A) The -log10 adjusted *P*-values of the top 20 GO Biological Processes (GeneSetDB Gene Ontology) by gene set enrichment analysis using EGSEA, sorted by average rank. There is enrichment for cell cycle and proliferation-related processes in the *NF1/PTPN11* wild-type (WT) cases (blue) relative to the cases with *NF1/PTPN11* alterations. (B) Normalized counts from RNA-sequencing data showing differences in *MKI67* transcript between the *NF1/PTPN11* altered and *NF1/PTPN11* WT groups. (C) Bar plot of the difference in proliferation index between the tumor subgroups by Ki67 immunohistochemistry. (D) Photomicrograph showing immunohistochemical expression of Ki67 in the tumor subgroups.

groups, as four of the five *NF1/PTPN11* samples subjected to unsupervised clustering were GI excisions. When we excluded genes associated with GI site from this tumor *versus* normal comparison, the two tumor subclusters were unaffected; however, a set of genes that were more clearly differentially expressed between the tumor subgroups were revealed that upon removal resulted in the elimination of the tumor subgroups. Functional enrichment of this set of genes using ToppFun (*https://toppgene.cchmc.org*) showed enrichment for cell cycle processes, supporting the EGSEA result and the interpretation that the observed clustering was related to the difference in cell cycle processes between tumor groups rather than the tumor site (*Online Supplementary Tables S6-S8* and *Online Supplementary Figures S6 and S7*).

Correlation of clonal IG rearrangement status and B-cell associated mutations with *NF1/PTPN11* wild-type status

Clonal analysis to detect rearrangements of IG and TRG genes was performed on 19 of 21 cases, including 6 of 7 *NF1/PTPN11* cases and 13 of 14 *NF1/PTPN11* wild-type cases. Five cases had clonal rearrangement of the IGH and/or the IGK locus [His04, His10, His14, His20, His21], while two cases (including one with IG rearrangement) showed rearrangements of the TRG locus [His13, His20]. One case was indeterminate for a significant clonal IG rearrangement [His12]. All five clonally rearranged cases for IG were *NF1/PTPN11* wild-type and all had additional mutations in transcriptional regulators and/or signaling pathway genes previously reported altered in B-cell lymphoma (see above). Three additional cases in the *NF1/PTPN11* wild-type group had at least one B-cell associated gene mutation [His07, His08 and His19]. IGH/*BCL2* (MBR) translocation analysis was positive in 1 of 17 cases [His10] (*Online Supplementary Table S3*). In total, 8 of the 14 cases in the *NF1/PTPN11* wild-type subgroup had clonal IG gene rearrangements or mutations in genes reported to be mutated in B-cell lymphomas (Figure 2).

Discussion

Our study furthers the current understanding of the genomic landscape of primary HS through integration of whole exome sequencing and gene expression analysis. It confirms the central role of the RAS/MAPK pathway in the pathogenesis of pHS, with RAS pathway abnormalities identified in all cases in this study. Moreover, it identifies

two molecular subgroups based on the presence or absence of *NF1/PTPN11* alterations and prevalence of *SETD2* mutations, and independently through unsupervised clustering of RNA-Seq data. In addition, our study identifies novel mechanisms of RAS/MAPK pathway activation, including a previously unreported intrachromosomal fusion between *TTYH3* and *BRAF* that preserves the BRAF kinase domain, and high-level *PTPN11* amplification. Perhaps the most surprising finding of our study was the discovery of the *NF1/PTPN11* subgroup with its distinct molecular characteristics and tissue site of involvement. In contrast to the *NF1/PTPN11* wild-type subgroup, none of these cases harbored abnormalities in genes associated with B-cell lymphomas beyond *SETD2* or had clonal IG rearrangements. GSEA revealed that this subgroup was characterized by a relative loss of gene sets related to cellular proliferation and the cell cycle compared to those harboring other RAS/MAPK alterations, a finding supported by Ki67 immunohistochemistry.

The majority of the *NF1/PTPN11* mutant cases had more than one MAPK pathway activating mutation. Three of the seven cases had co-occurring *NF1* and *PTPN11* mutations, while a fourth case had a co-occurring mutation in *GNAI2* involving a codon previously shown to activate the MAPK pathway.[29] Additionally, while the remaining *PTPN11* mutated case did not have a co-occurring *RAS* mutation, it did have high-level amplification of the mutated *PTPN11* allele. In *NF1* mutant melanoma, the frequent presence of a second gene mutation often involving *PTPN11* (or another RASopathy gene) has led to the suggestion that *NF1* inactivation is insufficient to cause full activation of the downstream MAPK pathway and tumorigenesis.[43] This hypothesis has been given further credence by recent data showing that *NF1* loss-of-function mutant cell lines are dependent on SHP2 (encoded by *PTPN11*) mediated signaling for oncogenic RAS/MAPK pathway activation,[44] raising the possibility that activating mutations of *PTPN11* may synergize with *NF1* loss-of-function mutations to further potentiate the oncogenic activity of the pathway.

In contrast to the *NF1/PTPN11* positive subgroup, the *NF1/PTPN11* wild-type cluster was comprised primarily of cases with prototypic RAS/MAPK pathway activating mutations involving *KRAS, NRAS, BRAF* and *MAP2K1*. Interestingly, eight of the 14 cases in this subgroup contained IG gene rearrangements and/or additional mutations in genes commonly associated with B-cell lymphoproliferative disorders. These included one or more mutations in epigenetic regulators, transcription factors or signaling pathway genes, including *CREBBP, KMT2D, DDX3X, ARID1A, MEF2B, SGK1, TNFRSF14, DTX1, GNA13, STAT6* and *CARD11*.[36-40] Clonal IG rearrangements were identified in five cases and a *BCL2* gene rearrangement was identified in one case, while neither were definitively detected in the *NF1/PTPN11* subgroup. In our series, it is worth noting that none of our cases had evidence of a concurrent or previous lymphoma, although we cannot exclude the possibility of an occult or unreported B-cell lymphoma being present. The finding of additional mutations associated with B-cell lymphomas and clonal IG gene rearrangements suggests that some cases of *NF1/PTPN11* wild-type pHS may be similar in origin to the sHS that are associated with B-cell malignancies, which often share IG gene rearrangements with the associated B-cell lymphoma.[5,6] This overlap has also been recently reported by Shanmugam *et al.*[18] In their series, they showed enrichment for a mutational signature resembling aberrant somatic hypermutation in cases that had a history of B-cell lymphoma or that had mutations in genes that are frequently mutated in B-cell lymphoma. Interestingly, they also found recurrent *CDKN2A* alterations that were more frequent in cases with a history of B-cell lymphoma or the aberrant somatic hypermutation signature. Similarly, our study identified a high frequency of focal *CDKN2A* losses/alterations in the *NF1/PTPN11* wild-type subgroup which, in our cohort, frequently had molecular alterations associated with B-cell lymphoma.

Concurrent mutations in RAS/MAPK pathway genes were less common in the *NF1/PTPN11* wild-type group, occurring in 4 of 14 cases with alterations. Two cases had concurrent mutations in *MAP2K1* [His11 and His14]. The other two had co-occurring *BRAF* (p.G469V) and *MAP2K1* (p.F53L) mutations [His10] or *KRAS* (p.G12D) and *RAF1* (p.D486G) mutations [His21]. These data are consistent with the limited published data in HS in which reported occurrences of multiple RAS/MAPK pathway mutations tend to manifest as co-occurring *MAP2K1* mutations[18] or involve atypical *BRAF* mutations, with co-occurring *BRAF* (p.G464V) and *KRAS* (p.Q61H),[45] *BRAF* (p.D594N) and *KRAS* (p.A146T),[18] *BRAF* (p.G469R) and *NF1* (p.W2229*)[18] and *BRAF* (p.F595L) and *HRAS* (p.Q61R) mutations[46] described. Interestingly, in the latter case the unusual *BRAF* mutation was shown to have weak oncogenic activity requiring the co-operation of the *HRAS* mutation for full activity.

Two of the analytical challenges in our study included the lack of available matched germline samples in all but three cases, and the possibility that over-representation of GI site in the *NF1/PTPN11* group could bias the RNA-Seq clustering. To exclude as many germline SNPs as possible we filtered all variants using stringent criteria for their representation in control populations (gnomAD)[47] and took CADD scores,[20] as well as presence in the Catalogue of Somatic Mutations in Cancer (COSMIC)[48] into consideration. In assessing potential site bias in gene expression clustering, we found that the separation of the tumor samples into the subgroups in the differential expression analysis was influenced by the removal of cell cycle-related genes but not by exclusion of GI site-associated genes. This, in addition to the similar mutational alterations in the cases, suggests that the clustering observed occurs independently of site.

In conclusion, our study provides further insight into the molecular pathogenesis of pHS. We show frequent mutations and alterations in genes of the RAS/MAPK pathway, suggesting that patients could potentially benefit from genomic evaluation and targeted therapy, and we report a distinct molecular subtype of pHS that correlates with the *NF1/PTPN11* status of the tumor and frequently involves the GI tract. Finally, we also identify a subset of *NF1/PTPN11* wild-type cases with mutations in B-cell lymphoma associated genes and/or clonal IG gene rearrangements. The identification of molecular subtypes of primary histiocytic sarcoma may prove to have clinical relevance in future studies.

Acknowledgments

The authors would like to thank Andrea O'Hara (BioDiscovery) and Karen Gustashaw (Thermo Fisher Scientific) for their assistance and software support in the interpretation of the OncoScan data; Arati Raziuddin, Xiaolin Wu, Jyoti Shetty, Bao Tran and Nina Bubunenko (Frederick National Laboratory for Cancer Research, Leidos Biomedical Research, Inc.) for per-

forming the library preparation, exome and RNA-Seq and OncoScan assay; Louis M. Staudt (Lymphoid Malignancies Branch, Center for Cancer Research, National Cancer Institute) for his critical reading of our manuscript.

Funding

This work was supported by the intramural research program of the Center for Cancer Research, National Cancer Institute, National Institutes of Health.

References

1. Swerdlow SH, Campo E, Harris NL, et al., eds. WHO Classification of Tumours of Haematopoietic and Lymphoid Tissues. Revised 4th Edition ed. Lyon, France: IARC, 2017.
2. Kommalapati A, Tella SH, Durkin M, Go RS, Goyal G. Histiocytic sarcoma: a population-based analysis of incidence, demographic disparities, and long-term outcomes. Blood. 2018;131(2):265-268.
3. Facchetti F, Pileri SA, Lorenzi L, et al. Histiocytic and dendritic cell neoplasms: what have we learnt by studying 67 cases. Virchows Arch. 2017;471(4):467-489.
4. Emile JF, Abla O, Fraitag S, et al. Revised classification of histiocytoses and neoplasms of the macrophage-dendritic cell lineages. Blood. 2016;127(22):2672-2681.
5. Feldman AL, Arber DA, Pittaluga S, et al. Clonally related follicular lymphomas and histiocytic/dendritic cell sarcomas: evidence for transdifferentiation of the follicular lymphoma clone. Blood. 2008;111(12):5433-5439.
6. Shao H, Xi L, Raffeld M, et al. Clonally related histiocytic/dendritic cell sarcoma and chronic lymphocytic leukemia/small lymphocytic lymphoma: a study of seven cases. Mod Pathol. 2011;24(11):1421-1432.
7. Feldman AL, Minniti C, Santi M, Downing JR, Raffeld M, Jaffe ES. Histiocytic sarcoma after acute lymphoblastic leukaemia: a common clonal origin. Lancet Oncol. 2004;5(4):248-250.
8. Soslow RA, Davis RE, Warnke RA, Cleary ML, Kamel OW. True histiocytic lymphoma following therapy for lymphoblastic neoplasms. Blood. 1996;87(12):5207-5212.
9. Alten J, Klapper W, Leuschner I, et al. Secondary histiocytic sarcoma may cause apparent persistence or recurrence of minimal residual disease in childhood acute lymphoblastic leukemia. Pediatr Blood Cancer. 2015;62(9):1656-1660.
10. Hure MC, Elco CP, Ward D, et al. Histiocytic sarcoma arising from clonally related mantle cell lymphoma. J Clin Oncol. 2012;30(5):e49-53.
11. Brunner P, Rufle A, Dirnhofer S, et al. Follicular lymphoma transformation into histiocytic sarcoma: indications for a common neoplastic progenitor. Leukemia. 2014;28(9):1937-1940.
12. Chen W, Lau SK, Fong D, et al. High frequency of clonal immunoglobulin receptor gene rearrangements in sporadic histiocytic/dendritic cell sarcomas. Am J Surg Pathol. 2009;33(6):863-873.
13. Hayase E, Kurosawa M, Yonezumi M, Suzuki S, Suzuki H. Aggressive sporadic histiocytic sarcoma with immunoglobulin heavy chain gene rearrangement and t(14;18). Int J Hematol. 2010;92(4):659-663.
14. Emile JF, Diamond EL, Helias-Rodzewicz Z, et al. Recurrent RAS and PIK3CA mutations in Erdheim-Chester disease. Blood. 2014;124(19):3016-3019.
15. Chakraborty R, Hampton OA, Shen X, et al. Mutually exclusive recurrent somatic mutations in MAP2K1 and BRAF support a central role for ERK activation in LCH pathogenesis. Blood. 2014;124(19):3007-3015.
16. Diamond EL, Durham BH, Haroche J, et al. Diverse and targetable kinase alterations drive histiocytic neoplasms. Cancer Discov. 2016;6(2):154-165.
17. Badalian-Very G, Vergilio JA, Degar BA, et al. Recurrent BRAF mutations in Langerhans cell histiocytosis. Blood. 2010; 116(11):1919-1923.
18. Shanmugam V, Griffin GK, Jacobsen ED, Fletcher CDM, Sholl LM, Hornick JL. Identification of diverse activating mutations of the RAS-MAPK pathway in histiocytic sarcoma. Mod Pathol. 2019;32(6):830-843.
19. Sondka Z, Bamford S, Cole CG, Ward SA, Dunham I, Forbes SA. The COSMIC Cancer Gene Census: describing genetic dysfunction across all human cancers. Nat Rev Cancer. 2018;18(11):696-705.
20. Rentzsch P, Witten D, Cooper GM, Shendure J, Kircher M. CADD: predicting the deleteriousness of variants throughout the human genome. Nucleic Acids Res. 2019;47(D1):D886-D894.
21. Robinson JT, Thorvaldsdottir H, Winckler W, et al. Integrative genomics viewer. Nat Biotechnol. 2011;29(1):24-26.
22. Alhamdoosh M, Ng M, Wilson NJ, et al. Combining multiple tools outperforms individual methods in gene set enrichment analyses. Bioinformatics. 2017;33(3):414-424.
23. Talevich E, Shain AH, Botton T, Bastian BC. CNVkit: genome-wide copy number detection and visualization from targeted DNA sequencing. PLoS Comput Biol. 2016; 12(4):e1004873.
24. Riester M, Singh AP, Brannon AR, et al. PureCN: copy number calling and SNV classification using targeted short read sequencing. Source Code Biol Med. 2016;11:13.
25. Kumar P, Henikoff S, Ng PC. Predicting the effects of coding non-synonymous variants on protein function using the SIFT algorithm. Nat Protoc. 2009;4(7):1073-1081.
26. Adzhubei IA, Schmidt S, Peshkin L, et al. A method and server for predicting damaging missense mutations. Nat Methods. 2010;7(4):248-249.
27. Kratz CP, Niemeyer CM, Castleberry RP, et al. The mutational spectrum of PTPN11 in juvenile myelomonocytic leukemia and Noonan syndrome/myeloproliferative disease. Blood. 2005;106(6):2183-2185.
28. Tajan M, de Rocca Serra A, Valet P, Edouard T, Yart A. SHP2 sails from physiology to pathology. Eur J Med Genet. 2015; 58(10):509-525.
29. Nairismagi ML, Tan J, Lim JQ, et al. JAK-STAT and G-protein-coupled receptor signaling pathways are frequently altered in epitheliotropic intestinal T-cell lymphoma. Leukemia. 2016;30(6):1311-1319.
30. Brown NA, Furtado LV, Betz BL, et al. High prevalence of somatic MAP2K1 mutations in BRAF V600E-negative Langerhans cell histiocytosis. Blood. 2014;124(10):1655-1658.
31. Frattini V, Trifonov V, Chan JM, et al. The integrated landscape of driver genomic alterations in glioblastoma. Nat Genet. 2013;45(10):1141-1149.
32. Johnston JJ, van der Smagt JJ, Rosenfeld JA, et al. Autosomal recessive Noonan syndrome associated with biallelic LZTR1 variants. Genet Med. 2018;20(10):1175-1185.
33. Tidyman WE, Rauen KA. Expansion of the RASopathies. Curr Genet Med Rep. 2016; 4(3):57-64.
34. Piotrowski A, Xie J, Liu YF, et al. Germline loss-of-function mutations in LZTR1 predispose to an inherited disorder of multiple schwannomas. Nat Genet. 2014;46(2):182-187.
35. Steklov M, Pandolfi S, Baietti MF, et al. Mutations in LZTR1 drive human disease by dysregulating RAS ubiquitination. Science. 2018;362(6419):1177-1182.
36. Karube K, Enjuanes A, Dlouhy I, et al. Integrating genomic alterations in diffuse large B-cell lymphoma identifies new relevant pathways and potential therapeutic targets. Leukemia. 2018;32(3):675-684.
37. Chapuy B, Stewart C, Dunford AJ, et al. Molecular subtypes of diffuse large B cell lymphoma are associated with distinct pathogenic mechanisms and outcomes. Nat Med. 2018;24(5):679-690.
38. Reddy A, Zhang J, Davis NS, et al. Genetic and Functional Drivers of Diffuse Large B Cell Lymphoma. Cell. 2017;171(2):481-494.e15.
39. Schmitz R, Wright GW, Huang DW, et al. Genetics and pathogenesis of diffuse large B-cell lymphoma. N Engl J Med. 2018; 378(15):1396-1407.
40. Landau DA, Sun C, Rosebrock D, et al. The evolutionary landscape of chronic lymphocytic leukemia treated with ibrutinib targeted therapy. Nat Commun. 2017; 8(1):2185.
41. Ross JS, Wang K, Chmielecki J, et al. The distribution of BRAF gene fusions in solid tumors and response to targeted therapy. Int J Cancer. 2016;138(4):881-890.
42. Ciampi R, Knauf JA, Kerler R, et al. Oncogenic AKAP9-BRAF fusion is a novel mechanism of MAPK pathway activation in thyroid cancer. J Clin Invest. 2005; 115(1):94-101.
43. Krauthammer M, Kong Y, Bacchiocchi A, et al. Exome sequencing identifies recurrent mutations in NF1 and RASopathy genes in sun-exposed melanomas. Nat Genet. 2015; 47(9):996-1002.
44. Nichols RJ, Haderk F, Stahlhut C, et al. RAS nucleotide cycling underlies the SHP2 phosphatase dependence of mutant BRAF-, NF1- and RAS-driven cancers. Nat Cell Biol. 2018;20(9):1064-1073.
45. Liu Q, Tomaszewicz K, Hutchinson L, Hornick JL, Woda B, Yu H. Somatic mutations in histiocytic sarcoma identified by next generation sequencing. Virchows Arch. 2016;469(2):233-241.
46. Kordes M, Roring M, Heining C, et al. Cooperation of BRAF(F595L) and mutant HRAS in histiocytic sarcoma provides new insights into oncogenic BRAF signaling. Leukemia. 2016;30(4):937-946.
47. Lek M, Karczewski KJ, Minikel EV, et al. Analysis of protein-coding genetic variation in 60,706 humans. Nature. 2016;536(7616):285-291.
48. Forbes SA, Beare D, Boutselakis H, et al. COSMIC: somatic cancer genetics at high-resolution. Nucleic Acids Res. 2017; 45(D1):D777-D783.